**Bulletin of Electrical Engineering and Informatics**
Vol. 13, No. 6, December 2024, pp. 3919~3927
ISSN: 2302-9285, DOI: 10.11591/eei.v13i6.7862 

# A novel high-gain DC-DC converter for photovoltaic applications

**Porselvi Thandavarayan, Arounassalame Mouttou**
Department of Electrical and Electronics Engineering, Puducherry Technological University, Puducherry, India

**Article Info**

***Article history:***

Received Nov 11, 2023
Revised Apr 9, 2024
Accepted May 17, 2024

***Keywords:***

DC-DC converter
Duty cycle
High-voltage gain applications
Photovoltaic system
Reduced gate driver circuits

**ABSTRACT**

This manuscript proposes a novel transformer-less, single-switch direct current (DC)-DC converter for renewable energy systems (RESs). The main aim is to solve the problems of low output voltage generated by photovoltaic (PV) arrays and discontinuous input supply current caused by switching mode power supplies. The new converter is a combination of a single-ended primary inductor, a diode/capacitor circuit, and a conventional quadratic boost converter. The main advantages are the higher rate of voltage conversion (more than 10 times for duty cycle above 50%), the diminished voltage across the active switch with diodes, and diminished gate driver necessity because of the use of a single switch with a continual input current for raising the PV panel life. Furthermore, the new converter produces low switching voltage, which improves system efficiency. The proposed converter operating principle and analysis based on steady-state performance are discussed. The proposed converter's performance is assessed using simulation in MATLAB/Simulink, and the results were presented. A 100 W prototype model of the designed DC-DC converter is also developed, and finally, the hardware results were compared with the simulated results.



***Corresponding Author:***

Porselvi Thandavarayan
Department of Electrical and Electronics Engineering, Puducherry Technological University
Puducherry, India
Email: porselvicget@gmail.com

## 1. INTRODUCTION

Nowadays, the choice of popular power generation system is photovoltaic (PV) power generation systems because of the reduction of carbon dioxide ($CO_2$) emissions and adaptation of the resources of clean energy. Apart from solar PV and solar heating systems, photons of energy from the sun are also helpful to humans indirectly in the form of biomass, wind energy, and hydropower, and have many advantages over traditional energy sources [1]–[3]. The production of power by the PV system is very low and it often depends on the weather conditions. A direct current (DC)-DC converter is connected between the solar array and the consumer end to reduce the number of solar PV panels and boost the voltage level [4]. Every solar array system now contained the maximum power point tracking (MPPT) algorithm to extract maximum power from PV arrays under fluctuating sun irradiation and load. An algorithm and electronic circuitry are used in the MPPT mechanism. Short circuit current approach, constant voltage, open-circuit voltage, incremental conductance, perturb and observe, fuzzy logic, neural network, genetic algorithm, and numerous MPPT algorithms are investigated. In this technique, for the maximum power transfer from PV source to load, the impedance matching condition should be satisfied. The tracked voltage of the PV system has a low voltage characteristic in nature and it has to be stepped up using a DC-DC converter [5]–[8].

Much research has been conducted in the field of power electronic DC-DC converters to meet industrial requirements, which is essential to raise the output voltage of PV systems to the desired level [9]. To stabilize the PV system power output, the duty ratio control of the switch in the power converter is required [10]. A standard boost converter is the primary choice for increasing the voltage output [11]. A high output voltage can be provided if the boost converter operates at an extreme duty cycle [12]. In addition, because of the converters practical internal parameters, very extreme duty cycles minimize the converters output voltage [13]. To increase the voltage gain, various research works provide different solutions and are categorized as converters that use magnetic coupling, magnetic coupling-free transformers [14]. Improvement in the turn ratio of higher frequency transformers will increase the voltage of high-frequency transformer-based converters [15]. Voltage spikes are induced by the transformer leakage inductance, which causes voltage spikes at active switches. Similarly, coupled inductor approach also suffers from voltage spikes due to transformer leakage inductance [16]. By employing a snubber circuit, the energy saved in leakage inductance is recycled but this circuit minimizes the efficiency of the converter [17]. Because of their simplicity and reduced size, converters that don't require magnetic coupling have recently gained greater interest among researchers [18]. The various transformer-less voltage boosting approaches like switched inductors and capacitors, voltage lifting multiplier cells are utilized in various DC-DC converters [19].

A modified voltage multiplier cell with switched inductors with the gain ratio six times the input voltage was proposed [20]. Here, the effectiveness of the converter was improved by less component count. An interleaved boost-single-ended primary-inductor converter (SEPIC) type DC-DC converter topology suitable for DC microgrid was proposed in [21]. This topology solves voltage imbalance problems in microgrid with less input current ripple but it employs more switches which makes control more complex. Bhaskar *et al.* [22] has suggested a non-inverting type converter incorporating symmetrical configuration multiplier cells to enhance output voltage gain. This makes the selection of components easier but the converter has reduced output voltage gain with the high component count. The non-isolated complete soft-switch boost converter suitable for renewable energy systems (RESs) applications was proposed in [23]. For the improvement of voltage gain, the proposed converter used a voltage multiplier cell with a three-winding coupled-inductor (TWCI) technique but it is suitable only for low power applications. A quasi-resonant higher gain higher efficiency single-ended primary inductor based DC-DC converter was proposed [24]. Here, switching power dissipations were minimized by soft-switching operation with the help of the quasi-resonance (QR) function applied to the middle capacitors and coupled inductor with increased semiconductor devices. Interleaved three winding CI DC-DC converters was proposed for fuel cell-based vehicles [25]. The low ripple current, as well as higher output voltage, were achieved by using inter-coupled gain cells connected in an input parallel with output series configuration the presented converter is better suited for high-voltage DC bus applications.

Numerous studies were already presented in the literature depending on power electronic devices for RESs utilizing certain methodologies with features. This paper proposes a transformer-less, high-gain converter to enhance the voltage generated by the PV system. The rest of the paper is organized as follows. Section 2 represents the standalone PV system configuration with the proposed converter. Section 3 illustrates the analysis of the new gain DC-DC converter. In section 4, the hardware and simulation outcomes with discussion are presented. Section 5 presents the conclusion.

## 2. PROPOSED CONVERTER METHOD

The new converter has a DC voltage source ($V_i$), main switch (S), five diodes as $D_1$, $D_2$, $D_3$, $D_4$, and $D_5$, three inductors as $L_1$, $L_2$, $L_3$, three capacitors as $C_1$, $C_2$, $C_3$, output diode ($D_0$), and output capacitor ($C_0$). The joined operation of the capacitors with source provides the charging of inductors $L_2$ and $L_3$ by capacitor $C_1$. Finally, the input source $V_g$, inductors $L_2$, $L_3$, and capacitor $C_2$, $C_3$ together release energy into the load in a series manner. The typical waveforms of the converter are shown in Figure 1which depicts the operation of the converter. The circuit diagram of the converter is shown in Figure 2. The proposed converter works in steady state with continuous conduction mode (CCM). In CCM, the inductor current flowing through the circuit never falls to zero. There are two operating modes during one switching period under CCM. Figure 3 depicts the equivalent circuits during metal oxide semiconductor field effect transistor (MOSFET) ON period (DT) and MOSFET OFF period (1-D) T and the current flow paths for these two operating modes. The operating modes are explained in detail as follows.

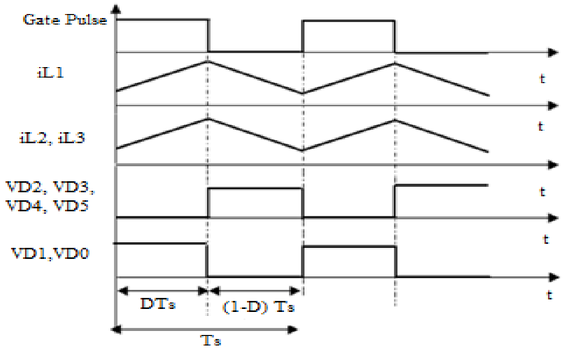


Figure 1. Theoretical waveforms of the proposed converter

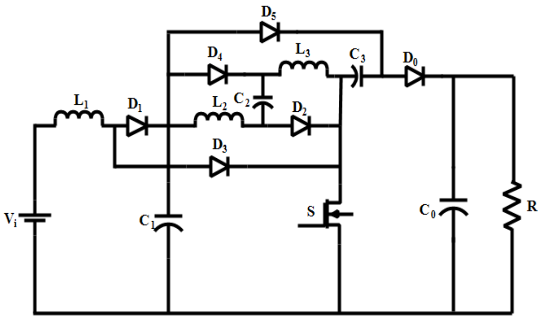


Figure 2. Circuit diagram of the proposed converter

## 3. METHOD

A DC-DC converter suitable for high voltage gain requirement can be designed efficiently by analysing the operating modes of the proposed circuit and voltage gain derivation.

### 3.1. Operating principle

Mode 1($0 \leq t \leq DT$): Figure 3(a) shows the circuit diagram of the proposed converter during mode 1 operation. During this operating period, when the MOSFET switch S is turned ON, the input voltage source magnetizes inductor $L_1$. The capacitor $C_1$ charges the inductors $L_2$, $L_3$, and capacitors $C_2$, $C_3$ in parallel. During this state, the inductor magnetizing currents $I_{L1}$, $I_{L2}$, and $I_{L3}$ gradually increase over time. Because the two inductors $L_2$ and $L_3$ are charged parallel by $C_1$, their currents are equal. The output capacitor $C_0$ discharges through the load resistance. Figure 3 depicts the six current flow paths in this mode. The following are the relevant equations:

$$V_{L1} = V_i \tag{1}$$

$$V_{L2} = V_{C1} \tag{2}$$

$$V_{L3} = V_{C1} \tag{3}$$

Mode 2($DT \leq t \leq T$): Figure 3(b) shows the circuit diagram of the proposed converter during mode 2 operation. During this operating period, the semiconductor switch S is turned OFF. The conducting diodes $D_1$ and $D_0$ are turned ON, whereas $D_2$, $D_3$, $D_4$, and $D_5$ are reverse biased. The inductors $L_1$, $L_2$, and $L_3$ are linearly demagnetized. Through diode $D_1$, the capacitor $C_1$ is charged from $L_1$. In series, the inductors $L_2$, $L_3$, and capacitors $C_2$, $C_3$ provide energy to the load. The output voltage is increased in this operation to attain the required gain transfer ratio. In this mode, Figure 3(b) shows 2 different current flow paths. The following are the associated equations:

$$V_{L1} = V_i - V_{C1} \tag{4}$$

$$V_{L2} = V_{C1} - V_{C2} + V_1 \tag{5}$$

$$V_{L3} = V_{C3} + V_1 - V_0 \tag{6}$$

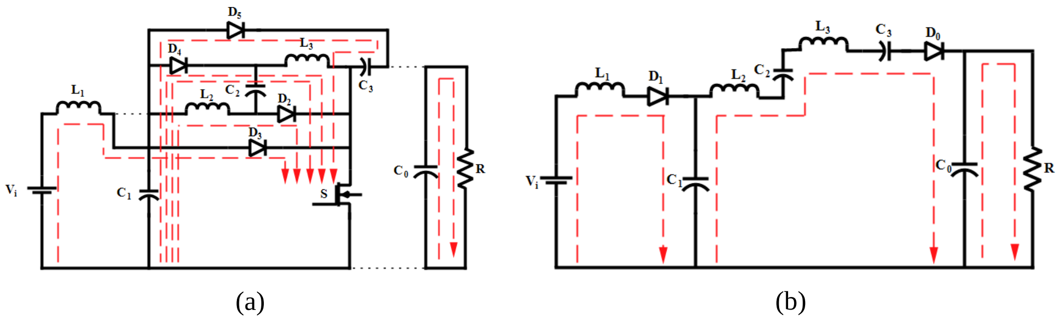


Figure 3. Circuit diagram; (a) during mode 1(0 ≤ t ≤ DT) and (b) during mode 2(DT ≤ t ≤ T)

### 3.2. Gain derivation

For a given switching period, the net changes in inductance currents are zero value under steady-state operating conditions.

$$\Delta i_{L,ON} - \Delta i_{L,OFF} = 0 \tag{7}$$

With respect to the dc source voltage $V_g$, the inductor current $i_{L1}$ increases linearly during the switch-on period (DT). Similarly, the current flowing in inductor $L_1$ decreases linearly with reference to the difference between input and capacitor $C_1$ voltage during the switch-off period. In (1) and (4) are used to calculate the value $i_{L1}$ during the on and off periods.

$$\Delta i_{L1\_ON} = \frac{V_i}{L_1} DT \tag{8}$$

$$\Delta i_{L1\_OFF} = \frac{(V_i - V_{C1})}{L_1} (1 - D)T \tag{9}$$

$$\frac{V_i}{L_1} DT + (1 - D)T \frac{(V_i - V_{C1})}{L_1} = 0 \tag{10}$$

$$V_{C1}(1 - D) = V_i \tag{11}$$

The inductor current $i_{L2}$ increases linearly depending on $V_C$ during switch ON period which is denoted as DT, whereas, the inductor current $i_{L2}$ decreases linearly depending on the capacitor $C_1$ and $C_2$ voltage during the switch OFF period which is denoted as (1-D)T. Hence, the value $i_{L2}$ during ON and OFF periods are expressed in (2) and (5):

$$\frac{V_{C1}}{L_2} DT + \frac{V_{C1} + V_{C2} - V_1}{L_2} (1 - D)T = 0 \tag{12}$$

$$\frac{V_{C1}}{L_3} DT + \frac{V_{C3} + V_1 - V_0}{L_3} (1 - D)T = 0 \tag{13}$$

$$\frac{V_i}{(1-D)} (3 - D) = (1 - D)V_0 \tag{14}$$

$$V_i(3 - D) = (1 - D)^2 V_0 \tag{15}$$

From (15), the voltage gain of the converter is expressed as (16):

$$\frac{V_0}{V_i} = \frac{(3-D)}{(1-D)^2} \tag{16}$$

### 3.3. Design of the passive components

The value of input inductor $L_1$ is designed by (17):

$$L_1 = \frac{R_0 (1-D)^4 D}{2(3-D) f_S} \tag{17}$$

Here, switching frequency is denoted as $f_s$, load resistance is denoted as $R_0$, output voltage is denoted as $V_0$, and duty ratio is denoted as D. The current flowing through inductors $L_2$ and $L_3$ are similar. The value of inductor $L_2$ is described as (18):

$$L_2 = \frac{R_0(1-D)^2 D}{2(3-D)f_s} \tag{18}$$

The capacitors voltage values is denoted as $V_C$ which is directly proportional to the output current, converter frequency and duty cycle. When the switch is in ON condition, the energy stored in the capacitors are described as (19) to (21):

$$C_1 = \left(\frac{4V_0 D}{(1-D)\Delta V_{C1} R_0 f_S}\right) \tag{19}$$

$$C_2 = C_3 = \left(\frac{DV_0}{\Delta V_{C2} R_0 f_S}\right) \tag{20}$$

$$C_0 = \left(\frac{DV_0}{\Delta V_{C0} f_S R_0}\right) \tag{21}$$

## 4. RESULTS AND DISCUSSION

This segment provides a detailed explanation of the simulation and hardware outcomes of the new high-gain converter. A novel transformer-less, single-switch, high output voltage gain converter for PV systems to solve the low voltage generated by solar PV systems and the intermittent input current generated due to changes in power supply by increasing the voltage level of the PV array was proposed. The new converter is the combination of diode–capacitor circuit and a conventional quadratic boost converter which produces higher output voltage with increased system efficiency.

The proposed novel DC-DC converter's laboratory model was built for 100 W. The proposed converter's results are evaluated using hardware and software outcomes, which confirms that the proposed converter is better suited for high-voltage applications. The prototype constructed is shown in Figures 4(a) and (b). Table 1 shows the parameters that were used in this laboratory model.

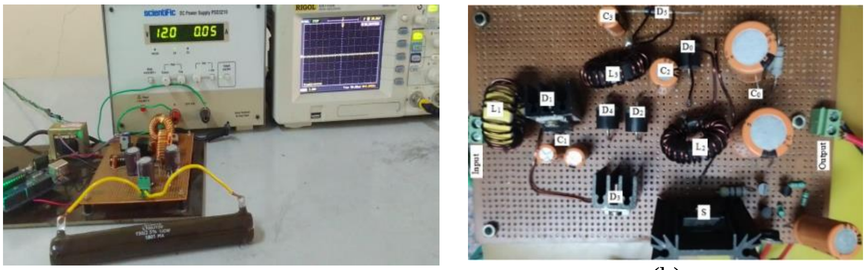

(a) (b)

Figure 4. Laboratory prototype; (a) connection of hardware setup and (b) components framework

Table 1. Selected system parameters for the novel converter

| Parameter | Value |
|---|---|
| Input voltage ($V_i$) | 12 V |
| Inductor ($L_1$) | 18 µH |
| Inductor ($L_2$ and $L_3$) | 72 µH |
| Capacitor 1 ($C_1$) | 70 µF |
| Capacitor ($C_2$) | 230 µF |
| Capacitor ($C_3$) | 70 µF |
| Power (W) | 100 W |
| Switching frequency ($f_s$) | 50 kHz |
| Load resistor (R) | 144 Ω |

The proposed converter simulation studies were done using MATLAB/Simulink. The current flowing through the inductors and output voltage waveforms are shown in Figure 5. The proposed converter is simulated for the input voltage of 12V and switching pulse of 0.5 duty ratio, as given in Figure 5(a) and (b) respectively. The current flowing via inductor $L_1$ is continuous and shown in Figure 5(c). The current flowing through $L_2$ and $L_3$ are continuous and remain stable throughout the switching period as shown in Figure 5(d).

The operation of the new high gain converter is analyzed and tested for varying duty cycles. For an input of 12 V, the output voltage is found to be 106 V while the duty ratio is 0.5, and Figure 5(e) represents this output voltage. Capacitor ripple is lesser than 0.5 V during the charging and discharge cycle. By further increasing the duty ratio to 0.6, the new converter output voltage increases to 160 V. Hence, it proves that the converter proposed is the best option for the higher output voltage applications.

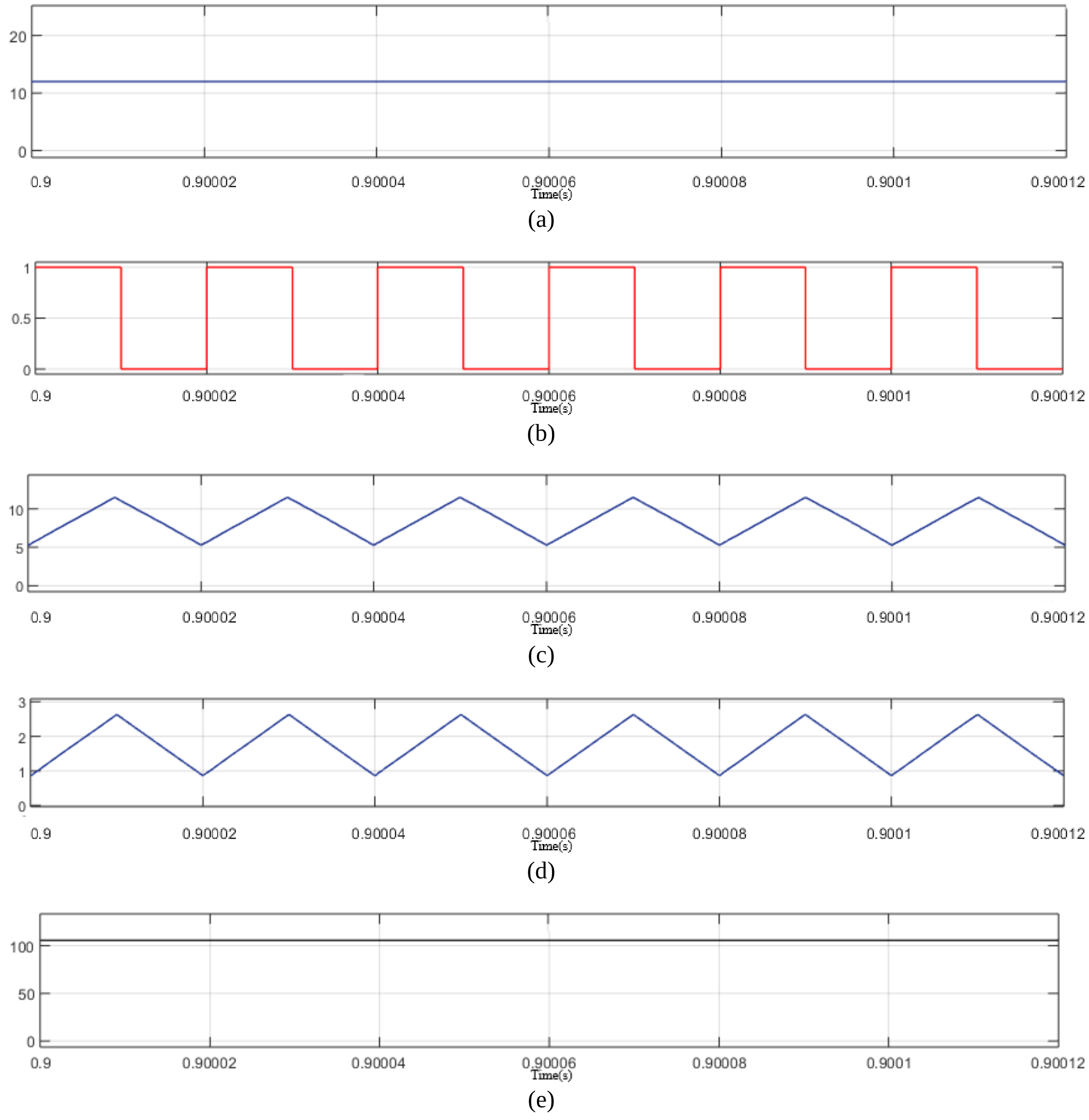


Figure 5. Simulation results; (a) input source voltage, (b) switching pulse waveform, (c) current flowing through $L_1$, (d) current flowing through $L_2$ and $L_3$, and (e) voltage across output capacitor $C_0$

The experimental outcomes of the proposed converter were given in Figures 6 and 7. The input inductor current $I_{L1}$ is continuous thereby safeguarding PV array lifetime and the current flowing through $L_2$ and $L_3$ are identical and are depicted in Figure 6(a). Figure 6(b) represents the experimental outcome of voltage stress across the switch and is given by 75 V. Figure 7(a) illustrates the voltage across capacitor $V_{C1}$

and is 30 V and $V_{C2}$ is 45 V. The experimental output voltage and current values are 160 V and 1.5 A for duty ratio 0.6 is shown in Figure 7(b).

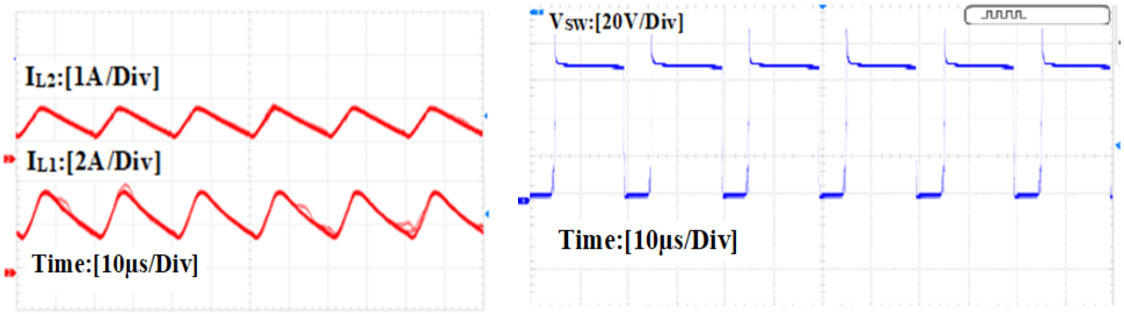


(a) (b)

Figure 6. Hardware results of the proposed converter; (a) current flowing across inductor $L_1$ and $L_2$ and (b) voltage across switch S

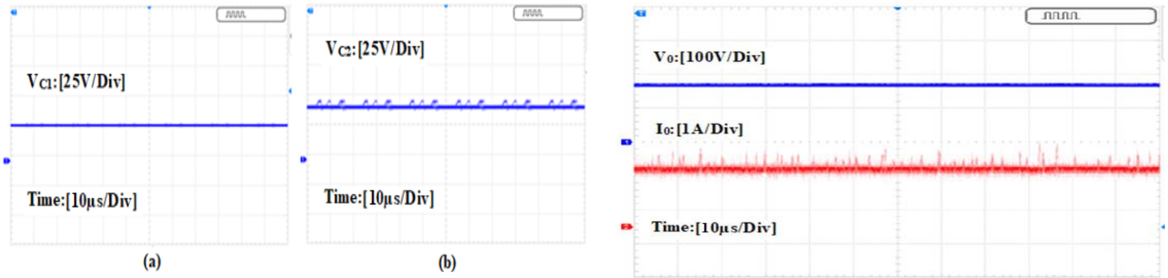


(a) (b)

Figure 7. Hardware results of the proposed converter; (a) voltage across the capacitor ((a) $V_{C1}$ and (b) $V_{C2}$) and (b) proposed converter output-voltage ($V_0$) and output-current ($I_0$)

Figure 8(a) shows the analysis of output voltage levels based on the duty cycle. At 50% duty ratio, the output voltage becomes 106 V. At 60% duty cycle, the output voltage becomes 165 V. From Figure 8(a), we can observe that increae in the duty cycle increases the output voltage of the circuit. Analysis of proposed converter efficiency is depicted in Figure 8(b). We can infer from the efficiency versus output power plot that for 70 W output power, the converter efficiency becomes 93.5%, the efficiency becomes 94% for 100 W output power, and so on. From this Figure 8(b), it is observed that the proposed converter efficiency can have maximum efficiency of 94.5%. Both simulation and hardware outcomes provide increased output voltage but a small difference is observed between them. Table 2 shows the performance comparion of the novel DC-DC converter with other existing topologies. In comparison to existing converters, the new converter provides a higher output voltage with fewer components, thereby reducing switch stress.

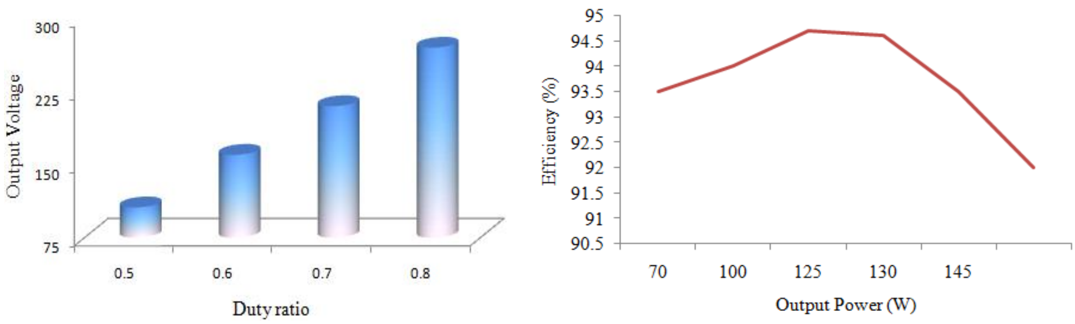


(a) (b)

Figure 8. Output performance; (a) analysis of output power based on the duty ratio and (b) efficiency of converter

Table 2. Recent performance study on the proposed high gain converter with available topologies

| Topology | Output voltage gain | Switching voltage stress /$V_o$ | Voltage stress across diodes/$V_o$ | Input inductor current | With common ground | Component count | | | |
|---|---|---|---|---|---|---|---|---|---|
| | | | | | | S | D | C | L |
| [10] | $3+D2/(1-D)$ | $(2M+1)/4M$ | $(2M+1)/4M$ | Non-pulsating | Yes | 1 | 4 | 4 | 2 |
| [26] | $(3-D)/(1-D)$ | $(M-1)/2M$ | $(M-1)/2M$ | Pulsating | No | 1 | 4 | 4 | 1 |
| [27] | $3/(1-D)$ | $1/3$ | $1/3$ | Continuous | Yes | 1 | 5 | 5 | 1 |
| [28] | $(1+2D)/(1-D$ | $(2+M)/3M$ | $(2+M)/3M$ | Continuous | Yes | 1 | 3 | 5 | 3 |
| [29] | $(2-D)/((1-D$ | $(2M)/\begin{matrix}(2M+1)\\+\sqrt{4M+1}\end{matrix}$ | $(2M)/\begin{matrix}(2M+1)\\+\sqrt{4M+1}\end{matrix}$ | Continuous | Yes | 1 | 4 | 3 | 2 |
| [30] | $(2+3D)/(1-D$ | $(M+3)/4M$ | $(M+3)/2M$ | Pulsating | No | 2 | 2 | 3 | 3 |
| Proposed converter | $(3-D)/(1-D)$ | $(M+3)/2M$ | $(M+3)/M$ | Continuous | Yes | 1 | 5 | 3 | 3 |

## 5. CONCLUSION

A novel-high-gain DC-DC converter useful for solar PV applications is proposed in this paper. The new converter provides higher voltage gain without using a coupled inductor or a transformer. The series-parallel charging and discharging of the converter passive elements reduces the switching voltage stress and low switch resistance. The performance of the proposed converter was tested using a prototype model built in the laboratory. To compare the performance of the proposed converter, simulation studies were also done. The simulation outcome demonstrates the output voltage as 160 V and also experimental results prove that the proposed converter is operated with maximum gain practically. The efficiency is analyzed under different duty cycles. Also, when the duty ratio is increased to 0.6, the proposed converter output is also increases and reaches a value of 160V. From the experimental outcomes, we can conclude that the proposed converter circuit is the better option for higher output voltage applications.

## ACKNOWLEDGEMENTS

The author would like to thank the Department of Science and Technology (DST)–INSPIRE Fellowship scheme for the financial support.

## REFERENCES

[1] N. Subhani, Z. May, M. K. Alam, I. Khan, M. A. Hossain, and S. Mamun, "An improved non-isolated quadratic DC-DC boost converter with ultra high gain ability," *IEEE Access*, vol. 11, pp. 11350–11363, 2023, doi: 10.1109/ACCESS.2023.3241863.

[2] D. Bao, A. Kumar, X. Pan, X. Xiong, A. R. Beig, and S. K. Singh, "Switched inductor double switch high gain DC-DC Converter for renewable applications," *IEEE Access*, vol. 9, pp. 14259–14270, 2021, doi: 10.1109/ACCESS.2021.3051472.

[3] S. Gopinathan, V. S. Rao, and K. Sundaramoorthy, "Family of non-isolated quadratic high gain DC-DC converters based on extended capacitor-diode network for renewable energy source integration," *IEEE Journal of Emerging and Selected Topics in Power Electronics*, vol. 10, no. 5, pp. 6218–6230, Oct. 2022, doi: 10.1109/JESTPE.2022.3167283.

[4] M. A. Salvador, T. B. Lazzarin, and R. F. Coelho, "High step-up DC-DC converter with active switched-inductor and passive switched-capacitor networks," *IEEE Transactions on Industrial Electronics*, vol. 65, no. 7, pp. 5644–5654, Jul. 2018, doi: 10.1109/TIE.2017.2782239.

[5] E. Koutroulis, K. Kalaitzakis, and N. C. Voulgaris, "Development of a microcontroller-based, photovoltaic maximum power point tracking control system," *IEEE Transactions on Power Electronics*, vol. 16, no. 1, pp. 46–54, Jan. 2001, doi: 10.1109/63.903988.

[6] T. Tafticht, K. Agbossou, M. L. Doumbia, and A. Chériti, "An improved maximum power point tracking method for photovoltaic systems," *Renewable Energy*, vol. 33, no. 7, pp. 1508–1516, Jul. 2008, doi: 10.1016/j.renene.2007.08.015.

[7] M. Lakshmi and S. Hemamalini, "Nonisolated high gain DC-DC converter for DC microgrids," *IEEE Transactions on Industrial Electronics*, vol. 65, no. 2, pp. 1205–1212, Feb. 2017, doi: 10.1109/TIE.2017.2733463.

[8] Y. Wang, Y. Qiu, Q. Bian, Y. Guan, and D. Xu, "A single switch quadratic boost high step up DC-DC converter," *IEEE Transactions on Industrial Electronics*, vol. 66, no. 6, pp. 4387–4397, Jun. 2019, doi: 10.1109/TIE.2018.2860550.

[9] A. A. Fardoun and E. H. Ismail, "Ultra step-up DC-DC converter with reduced switch stress," *IEEE Transactions on Industry Applications*, vol. 46, no. 5, pp. 2025–2034, Sep. 2010, doi: 10.1109/TIA.2010.2058833.

[10] B. Wu, S. Li, Y. Liu, and K. Ma Smedley, "A new hybrid boosting converter for renewable energy applications," *IEEE Transactions on Power Electronics*, vol. 31, no. 2, pp. 1203–1215, Feb. 2016, doi: 10.1109/TPEL.2015.2420994.

[11] M. Forouzesh, Y. P. Siwakoti, S. A. Gorji, F. Blaabjerg, and B. Lehman, "Step-up DC-DC converters: a comprehensive review of voltage-boosting techniques, topologies, and applications," *IEEE Transactions on Power Electronics*, vol. 32, no. 12, pp. 9143–9178, Dec. 2017, doi: 10.1109/TPEL.2017.2652318.

[12] M. Muhammad, M. Armstrong, and M. A. Elgendy, "A nonisolated interleaved boost converter for high-voltage gain applications," *IEEE Journal of Emerging and Selected Topics in Power Electronics*, vol. 4, no. 2, pp. 352–362, Jun. 2016, doi: 10.1109/JESTPE.2015.2488839.

[13] X. Hu, J. Wang, L. Li, and Y. Li, "A three-winding coupled-inductor DC-DC converter topology with high voltage gain and reduced switch stress," *IEEE Transactions on Power Electronics*, vol. 33, no. 2, pp. 1453–1462, Feb. 2018, doi: 10.1109/TPEL.2017.2689806.

[14] T. D. Duong, M. K. Nguyen, T. T. Tran, Y. C. Lim, and J. H. Choi, "Transformerless high step-up DC-DC converters with switched-capacitor network," *Electronics (Switzerland)*, vol. 8, no. 12, p. 1420, Nov. 2019, doi: 10.3390/electronics8121420.

[15] M. Maalandish, S. H. Hosseini, S. Ghasemzadeh, E. Babaei, R. S. Alishah, and T. Jalilzadeh, "Six-phase interleaved boost dc/dc converter with high-voltage gain and reduced voltage stress," *IET Power Electronics*, vol. 10, no. 14, pp. 1904–1914, Nov. 2017,

doi: 10.1049/iet-pel.2016.1029.
[16] Z. Chen, Q. Zhou, and J. Xu, "Coupled-inductor boost integrated flyback converter with high-voltage gain and ripple-free input current," *IET Power Electronics*, vol. 8, no. 2, pp. 213–220, Feb. 2015, doi: 10.1049/iet-pel.2014.0066.
[17] S. Zhuo, A. Gaillard, L. Guo, L. Xu, D. Paire, and F. Gao, "Active disturbance rejection voltage control of a floating interleaved DC-DC boost converter with switch fault consideration," *IEEE Transactions on Power Electronics*, vol. 34, no. 12, pp. 12396–12406, Dec. 2019, doi: 10.1109/TPEL.2019.2905897.
[18] L. S. Yang, T. J. Liang, H. C. Lee, and J. F. Chen, "Novel high step-up DC-DC converter with coupled-inductor and voltage-doubler circuits," *IEEE Transactions on Industrial Electronics*, vol. 58, no. 9, pp. 4196–4206, Sep. 2011, doi: 10.1109/TIE.2010.2098360.
[19] G. Wu, X. Ruan, and Z. Ye, "Nonisolated high step-up DC-DC converters adopting switched-capacitor cell," *IEEE Transactions on Industrial Electronics*, vol. 62, no. 1, pp. 383–393, Jan. 2015, doi: 10.1109/TIE.2014.2327000.
[20] H. Li, H. Du, Y. Zeng, Z. Qiu, X. Jiang, and Z. Chen, "A modified interleaved capacitor clamped DC-DC converter with non-resonant soft switching," *IEEE Transactions on Power Electronics*, vol. 37, no. 10, pp. 12221–12236, Oct. 2022, doi: 10.1109/TPEL.2022.3163010.
[21] P. Prabhakaran and V. Agarwal, "Novel boost-SEPIC type interleaved DC-DC Converter for mitigation of voltage imbalance in a low-voltage bipolar DC microgrid," *IEEE Transactions on Industrial Electronics*, vol. 67, no. 8, pp. 6494–6504, Aug. 2020, doi: 10.1109/TIE.2019.2939991.
[22] M. S. Bhaskar, M. Meraj, A. Iqbal, and S. Padmanaban, "Nonisolated symmetrical interleaved multilevel boost converter with reduction in voltage rating of capacitors for high-voltage microgrid applications," *IEEE Transactions on Industry Applications*, vol. 55, no. 6, pp. 7410–7424, Nov. 2019, doi: 10.1109/TIA.2019.2936178.
[23] S. Habibi, R. Rahimi, M. Ferdowsi, and P. Shamsi, "A high step-up DC-DC converter using a three winding coupled inductor for photovoltaic to grid applications," in *2022 IEEE Energy Conversion Congress and Exposition, ECCE 2022*, Oct. 2022, pp. 1–6, doi: 10.1109/ECCE50734.2022.9948055.
[24] S. Hasanpour, M. Forouzesh, Y. Siwakoti, and F. Blaabjerg, "A new high-gain, high-efficiency SEPIC-based DC–DC converter for renewable energy applications," *IEEE Journal of Emerging and Selected Topics in Industrial Electronics*, vol. 2, no. 4, pp. 567–578, Oct. 2021, doi: 10.1109/jestie.2021.3074864.
[25] H. Li, C. Li, X. Sun, L. Cheng, and W. Li, "An interleaved high step-up DC/DC converter-based three-winding coupled inductors with symmetrical structure," *IEEE Transactions on Power Electronics*, vol. 38, no. 5, pp. 6642–6652, May 2023, doi: 10.1109/TPEL.2023.3244809.
[26] J. C. Rosas-Caro, J. M. Ramirez, F. Z. Peng, and A. Valderrabano, "A DC-DC multilevel boost converter," *IET Power Electronics*, vol. 3, no. 1, pp. 129–137, 2010, doi: 10.1049/iet-pel.2008.0253.
[27] N. Elsayad, H. Moradisizkoohi, and O. A. Mohammed, "A single-switch transformerless DC-DC converter with universal input voltage for fuel cell vehicles: analysis and design," *IEEE Transactions on Vehicular Technology*, vol. 68, no. 5, pp. 4537–4549, May 2019, doi: 10.1109/TVT.2019.2905583.
[28] M. Chen, K. Li, J. Hu, and A. Ioinovici, "Generation of a family of very high DC gain power electronics circuits based on switched-capacitor-inductor cells starting from a simple graph," *IEEE Transactions on Circuits and Systems I: Regular Papers*, vol. 63, no. 12, pp. 2381–2392, Dec. 2016, doi: 10.1109/TCSI.2016.2606124.
[29] L.-S. Yang and J.-H. Cai, "High step-up DC-DC converter with switched multi-inductor technique," *International Journal of Electrical Energy*, vol. 7, no. 1, pp. 15–20, Jun. 2019, doi: 10.18178/ijoee.7.1.15-20.
[30] Y. Tang, D. Fu, T. Wang, and Z. Xu, "Hybrid switched-inductor converters for high step-up conversion," *IEEE Transactions on Industrial Electronics*, vol. 62, no. 3, pp. 1480–1490, Mar. 2015, doi: 10.1109/TIE.2014.2364797.

## BIOGRAPHIES OF AUTHORS

**Porselvi Thandavarayan** received the B.Tech. degree in Electrical and Electronics Engineering in 2013 and M.Tech. degree in Green Energy Technology (Gold Medalist) in 2015 from Pondicherry University, India. Currently, she is doing Ph.D. in Puducherry Technological University, Puducherry, India. She can be contacted at email: porselvicget@gmail.com.

**Arounassalame Mouttou** received the B.Tech. degree from Pondicherry University, India in 1993 and M.Tech. degree from University of Calicut, India in 1998. He received the Ph.D. degree in Systems and Control Engineering from IIT Bombay, India in 2009. Presently, he is working as Professor at the Department of Electrical and Electronics Engineering, Puducherry Technological University, Puducherry, India. He can be contacted at email: arun@ptuniv.edu.in.